

# STUDY OF COPPER MICROSTRUCTURE PRODUCED BY ELECTROFORMING FOR THE 180-GHz FREQUENCY CORRUGATED WAVEGUIDE\*

K. Suthar<sup>†</sup>, G. Navrotski, P. Carriere<sup>1</sup>, and A. Zholents  
Argonne National Laboratory, Lemont, IL, USA  
<sup>1</sup>RadiaBeam Inc., Santa Monica, CA, USA

## Abstract

Fabrication of the corrugated structure that generates a field gradient of  $100 \text{ MV m}^{-1}$  at 180 GHz is a challenge, requiring unconventional manufacturing methods. The corrugated waveguide with 2-mm-inner-diameter will be produced by electroplating copper on the aluminum mandrel as proposed in [1]. A thin seed layer is usually applied to achieve uniform wetting of the plated copper on the aluminum mandrel. The copper waveguide is retrieved by removing the mandrel. Uniform copper plating and etching of the aluminum are crucial steps to keep the surface uniformly smooth and free of impurities that are especially necessary for the vacuum RF application. Previous studies suggest that electroplated copper has variations in both electrical and mechanical properties compared with those of bulk copper from batch production. In this paper we discuss the copper microstructure produced by the electroforming method and a literature study on variations, which can be attributed to disparity in the crystalline grain structure of the plated material.

## INTRODUCTION

A 0.5-m-long, 1 mm internal radius, miniature cylindrical corrugated waveguide accelerator (CWA) is being proposed [2] and designed to create sub-terahertz Čerenkov radiation produced by an electron bunch traveling longitudinally on the centerline of the corrugated waveguide [1]. The dimensions of the corrugated structure are shown in Fig. 1. While the RF design [3] and prototype fabrication efforts are under development [4], we are investigating the limits of operating conditions based on the heat transfer and mechanical robustness of the structure during operation via fully coupled multiphysics finite element analyses.

The corrugated structure operates at 180 GHz with a transformer ratio of 5 that can deposit about 600 W of heat load at 10 kHz repetition rate on the inner surface of the corrugation and the transition section. The RF-heat-load deposition increases along the length of the structure producing a temperature gradient that can generate progressively higher thermal expansion in the downstream direction. Estima-

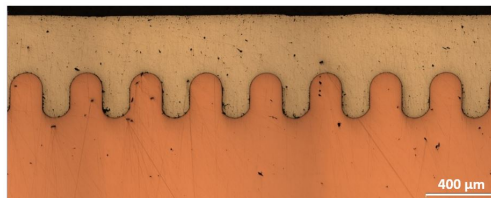


Figure 1: A micrograph of a section of the copper corrugated waveguide on an aluminum forming mandrel.

tion of unavoidable fabrication errors and the differential dimensional changes due to thermal expansion are crucial for achieving the required performance from the corrugated waveguide. The resulting thermal stress from the differential thermal expansion can lead to tensile-yield failure. Such failure can generate arcing due to surface cracking that ultimately causes loss of the beam. Operating parameters, such as energy and repetition rate, are the deciding factors for how much energy and how fast heat will be deposited on the structure. Therefore, fabrication acceptance criteria are also critical in reducing the beam instabilities that are potentially caused by fabrication errors. To quantify such behavior and to evaluate the mitigation scheme in the high-frequency structure, we are investigating the thermal budget for the structure via careful and detailed finite element analyses [1].

## ANALYSIS

### The Geometry

The corrugated waveguide geometry is shown in Fig. 1, and further details can be found in [4]. The CWA length with the corrugated waveguide is 0.5 m.

Table 1: Dimensions of Corrugation

Dimension	Value
$a$ - Waveguide inner radius)	1 mm
$d$ - Corrugation depth	263 $\mu\text{m}$
$t$ - Corrugation tooth width	160 $\mu\text{m}$
$v$ - Corrugation spacing	340 $\mu\text{m}$
$r$ - Corrugation corner radius	80 $\mu\text{m}$

### Fabrication Considerations

The corrugated waveguide is produced by electroplating copper on an aluminum mandrel. A thin seed layer of copper, measuring  $2.0 \pm 0.5 \mu\text{m}$  in thickness is usually applied

\* This research used resources of the Advanced Photon Source, a U.S. Department of Energy (DOE) Office of Science User Facility and is based on work supported by Laboratory Directed Research and Development (LDRD) funding from Argonne National Laboratory, provided by the Director, Office of Science, of the U.S. DOE under Contract No. DE-AC02-06CH11357.

<sup>†</sup> suthar@anl.gov

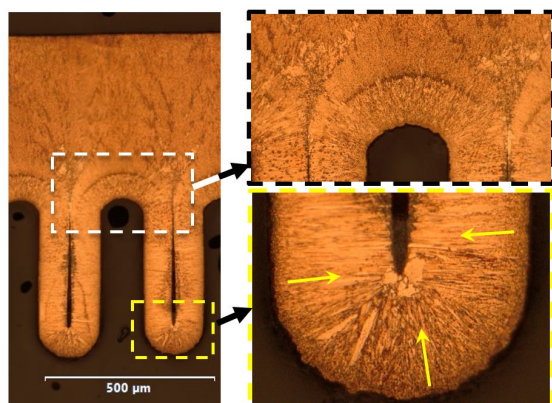


Figure 2: Cross section of an early prototype of an electroformed copper waveguide. (left) Etched microstructure of two corrugations. (top right) Magnified view of the corrugation root radius showing the dramatic change in crystalline morphology at the ‘pinch point’ where copper grains from adjacent corrugations collide, resulting in the creation of a central void along the convolution axis. (bottom right) Magnified view of the waveguide inner diameter corrugation radius with highly directional, acicular crystalline growth highlighted by yellow arrows.

to achieve uniform wetting of the aluminum mandrel. Bulk copper is subsequently layered by electroplating until the full thickness of the component has been achieved. The completed copper waveguide is retrieved by chemical dissolution of the aluminum mandrel. Preparation of the mandrel, uniform copper plating of the seed layer, electrodeposited growth of the bulk component, and the subsequent removal of the aluminum mandrel are all crucial steps to produce a waveguide with vacuum-side surfaces that are smooth, uniform, and free of impurities, which are especially necessary for corrugated waveguide accelerators. In addition, previous studies suggest that electroplated copper has variations in both electrical and mechanical properties compared with those of bulk copper from batch production. These variations can be attributed to disparities of the crystalline grain structure in plated material [5].

In an electroplating bath the deposition of copper atoms follows the lines of electrical potential. As a result, the grain growth direction is perpendicular to the surface being plated, in this case, an aluminum mandrel surface. The dynamic growth process can be impeded by changes in the geometry and flow of electrolytes. This leads to variation in growth rate, size, and orientation of the grain structure as can be seen in Fig. 2.

Porous or sparse grain boundaries can decrease thermal conductivity, increase electrical resistivity, and produce variations in mechanical strength at various locations. Defects on the mandrel surface act as templates for future copper electroformation. These mandrel defects imprint into the structure as shown in Fig. 3. Small machining marks on the aluminum mandrel surface, inadvertent scratches from handling, or shallow pitting created during cleaning form

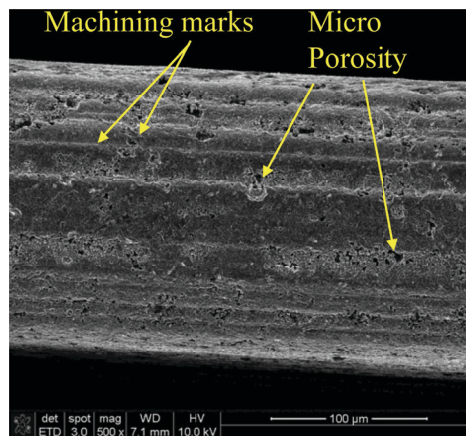


Figure 3: Defects in electroplated copper.

a template that is duplicated in the electroforming process. Combining material history, achievable fabrication tolerances, and electromagnetic heating lead to dimension uncertainty to a high level of concern that necessitates rigorous investigation into the thermal stress and resulting expansion.

## RESULTS

### *Microstructural Observations*

Building upon experience gained with initial prototypes, the current waveguide design is shown in cross section in Fig. 4 with the geometry outlined in Table 1. The microstructure shows natural variations in color highlighted by etching with a ferric nitrate and nitric acid solution. A magnified image highlighting the fine structure of one corrugation is shown in the upper right. Following the crystal morphology from bottom to top in the image: each corrugation begins with a 3- $\mu\text{m}$  seed crystal skin followed by (1) a small cluster of large, equiaxed grains at the apex of each corrugation. This grouping represents the lightest colored and lowest strength material in the composite system. Following in conformation to the seed layer is (2), a layer composed of highly elongated, single-crystal grains aligned with their long axes oriented perpendicular to the growth mandrel interface. Regions (3) and (4) complete the distinct interior core of the electroformed waveguide with region (3) having a more amorphous character and region (4) exhibiting a degree of recrystallization preferentially oriented out and away from layer (2). Region (5), the darkest, most amorphous, and hardest region of the component, may be the byproduct of a planned change in chemical electrodeposition conditions to increase the growth rate of the component. Region (6) is farthest removed from the initial electroplating template and exhibits the same nascent recrystallization characteristics as region (4), except that the nucleation source of region (6)’s recrystallization process started at the outer surface of the waveguide. Unlike the interface between regions (4) and (5), there is no distinct change in mechanical properties (microhardness) between regions (5) and (6).

The microstructure of electrodeposited copper is unique due to the assembly of atoms at room temperature via chem-

Content from this work may be used under the terms of the CC BY 3.0 licence (© 2021). Any distribution of this work must maintain attribution to the author(s), title of the work, publisher, and DOI

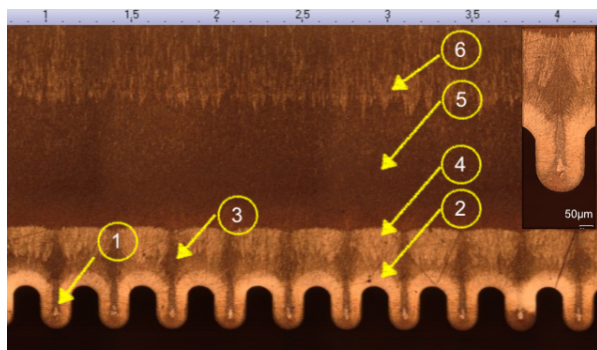


Figure 4: Cross section of an electroformed copper waveguide tube with improved geometry. See text for a detailed explanation of the numbered regions.

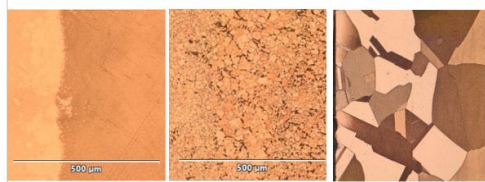


Figure 5: Comparison of microstructures: (left) As fabricated electrodeposit, (center) fully annealed microstructure, and (right) typical high conductivity copper.

ical methods that hinder the growth of crystallites and thus produce an atypical grain structure in the metal (see Fig. 5). Even at highest practical optical magnification, the electroformed copper remains uniform and featureless except for the distinct interface between dark and light regions that indicates a material change [noted as region (4) in Fig. 4]. When fully annealed, the microstructure recrystallizes, and grains grow to roughly  $8\ \mu\text{m}$  in diameter (Fig. 5, center image) with void coalescence at the grain boundaries. For comparison, a typical microstructure of oxygen-free copper (UNS C10100) is shown in the right image.

### Microhardness Measurements

Average microhardness measured across this waveguide was Vickers  $\text{HV} = 170 \pm 25\ \text{kgf/mm}^2$ , which is equivalent to an ultimate tensile strength (UTS) of approximately 500 MPa. This surpasses the strength of GlidCop® (UNS C15715) [6] and copper-chromium-zirconium (UNS C18150) at the expense of being brittle and highly sensitive to fracture at stress concentrations [7]. At the other extreme, this component material can be fully annealed to  $\text{HV} 29\ \text{kgf/mm}^2$ , equivalent to a UTS near 90 MPa with recovery of maximum ductility.

### Microroughness Measurements

These convolutions interact with the wakefield of the electron bunch being accelerated along the central axis of the device. The quality of the electroformed interior surface duplicates the quality of the aluminum mandrel template at sub-micrometer scales. For this prototype, average surface roughness of the interior convolutions is measured  $R_A =$

$6\ \mu\text{m}$ . A high temperature anneal, equivalent to subjecting the waveguide to a brazing cycle, reduces the average roughness by 30% by smoothing the highest roughness peaks at the expense of coarsening the overall roughness profile.

### Electrical Conductivity Measurements

The transport properties, i.e., electrical and thermal conductivity, are crucial in defining the performance of the wakefield accelerator. Four witness coupons, 10 mm in diameter and  $500\ \mu\text{m}$  thick, were included in the waveguide plating bath. The electrical conductivity was measured using a 480 kHz SigmaScope SMP10 eddy current probe according to ASTM E1004 [8]. The electrical conductivity of the electroplated copper is equal to about  $88 \pm 2\%$  of the International Annealed Copper Standard (IACS), wherein 100% IACS is  $58.108\ \text{MS/m}$  at  $20\ ^\circ\text{C}$ . The corresponding skin depth is estimated to be  $88\ \mu\text{m}$ , which is much smaller than the sample thickness. The 2% uncertainty is derived from prior benchmarking tests performed on various copper grades, wherein the SMP10 eddy current results were compared against more accurate 4-probe measurements performed according to ASTM B193 [9]. Further through-thickness validation is required, as the eddy current method only samples the uppermost layer of the copper.

## SUMMARY

Electroforming of components can be a high-precision and cost-effective method of producing complex parts. This study has examined the underlying material properties that affect component physical and mechanical performance in a unique accelerator application. The electroplated copper showed directional growth of grains. After annealing, it was observed that the grains grew in size, leaving large void spaces between clusters of grains. While the surface roughness study inferred that the peaks formed due to smaller grains after the electroplating process, they were modulated after annealing at  $750\ ^\circ\text{C}$  for 30 minutes. Therefore, the average surface roughness has not improved significantly. Moreover, the mechanical hardness property measurements showed a higher hardness value for the electroplated copper; however, that reduced significantly after annealing the same sample. Similarly, the electrical conductivity measurement showed about 12% reduction compared to the IACS standard. We conclude that the researcher should exercise great care using electroformed components in applications using high vacuum and high frequency electromagnetic fields.

## FUTURE WORK

We are planning to conduct a thorough investigation to study the electroformed waveguide for the A-STAR project at Argonne National Laboratory. An investigation is in progress to determine how to improve the metallurgy to increase thermal and electrical conductivity and achieve better dimensional tolerances. One of the main goals of our research is to decrease surface roughness. Researchers are

welcome to send their comments and suggestions regarding this topic to the authors of the paper.

## REFERENCES

- [1] A. Zholents *et al.*, “A conceptual design of a compact wake-field accelerator for a high repetition rate multi user x-ray free-electron laser facility,” in *Proc. IPAC’18*, Vancouver, BC, Canada, Jun. 2018, pp. 1266–1268. doi: 10.18429/JACoW-IPAC2018-TUPMF010.
- [2] A. A. Zholents and W. M. Fawley, “Proposal for intense attosecond radiation from an X-ray free-electron laser,” *Phys. Rev. Lett.*, vol. 92, no. 22, p. 224 801, Jul. 2004. doi: 10.1103/PhysRevLett.92.224801.
- [3] G. Waldschmidt *et al.*, “Design and test plan for a prototype corrugated waveguide,” in *Proc. IPAC’18*, Vancouver, BC, Canada, Jun. 2018, pp. 1550–1552. doi: 10.18429/JACoW-IPAC2018-TUPML009.
- [4] K. Suthar *et al.*, “Investigation of various fabrication methods to produce a 180GHz corrugated waveguide structure in 2mm-diameter 0.5m-long copper tube for the compact wakefield accelerator for FEL facility,” in *Proc. NAPAC’19*, Lansing, MI, USA, Oct. 2019, pp. 286–289. doi: 10.18429/JACoW-NAPAC2019-MOPL023.
- [5] N. Murata *et al.*, “Micro texture dependence of the mechanical and electrical reliability of electroplated copper thin film interconnections,” in *Proc. 2011 IEEE 61st Electronic Components and Technology Conference (ECTC)*, May 2011, pp. 2119–2125. doi: 10.1109/ECTC.2011.5898811.
- [6] “GLIDCOP AL-15: dispersion-strengthened copper,” *Alloy Digest*, vol. 45, no. 5, 1996. doi: 10.31399/asm.ad.cu0603.
- [7] G. Navrotski, internal communication, 2019.
- [8] ASTM, “Standard test method for determining electrical conductivity using the electromagnetic (eddy current) method,” ASTM International, Tech. Rep. E1004-17, 2017. doi: 10.1520/E1004-17.
- [9] ASTM, “Standard test method for resistivity of electrical conductor materials,” ASTM International, Tech. Rep. B193-19, 2019. doi: 10.1520/B0193-19.